Enhanced Second-Harmonic Generation in AlGaAs Nanoantennas

L. Carletti[1], D. Rocco[1], A. Locatelli[1], C. De Angelis[1]

[1]University of Brescia, Italy

Abstract

Introduction
In the last two decades, we assisted to an exponentially increasing interest in nanometallic objects based on plasmonic resonances due to a huge range of applications such as surface enhanced fluorescence [1], surface enhanced Raman scattering [2], solar cells [3], and nanomedicine [4]. However, metals suffer from large resistive heating losses in the visible and near-infrared (near-IR) wavelength range, which limit device performance [5,6]. In contrast to plasmonic antennas, the optical response of dielectric particles does not suffer from ohmic losses and can exhibit both strong electric and magnetic optical resonances in the visible and near-IR wavelength range [7,8]. These optical properties make all-dielectric nanoantennas a unique opportunity for the study of nonlinear optical effects generated from both electric and magnetic resonances [9].

Use of COMSOL Multiphysics®
We investigated the scattering characteristics of Al0.18Ga0.82As cylinders at near-IR wavelengths by using Frequency Domain (FD) simulations in the Wave Optics Module. We run FD simulations using either a plane wave excitation or an electric dipole point source. The scattered field was finally decomposed in a multipolar expansion [9].

In order to investigate the SHG phenomenon, we used the nonlinear polarization induced by $\chi(2)$ as a source in subsequent FD simulations. First we solved the linear electromagnetic problem at the fundamental frequency (FF). Then we used the calculated fields to define the SH source as external current density and solved the problem at the second harmonic (SH) frequency ωSH, in analogy to [10]. The i-th component of the external current density Ji was expressed as
$Ji = j*\omega SH*\varepsilon 0*\chi(2)*EFF,j*EFF,k$, $i \neq j \neq k$
where $\varepsilon 0$ is the vacuum permittivity and EFF,i is the i-th component of the electric field at the FF.

Results
The scattering efficiency calculated for a cylinder suspended in air with radius r=225 nm and height h=400 nm is shown in Figure 1. The resonance observed at λ=1640 nm is a magnetic dipole resonance, as it can be inferred from the electric field distribution shown in Figure 1. By increasing the cylinder radius, the resonances red-shift in wavelength (see Figure 2).

The calculated SHG efficiency for a cylinder suspended in air is shown in Figure 3. The maximum SHG efficiency is obtained for a pump wavelength of λ=1675 nm. This is due to the presence of a mode with a significant spatial overlap with the pump mode.
Figure 4 provides the SHG efficiency as a function of pump wavelength and cylinder radius. The peak wavelength of SHG efficiency red-shifts as the radius of the cylinder is increased, following the resonant mode at the emission wavelength that was found to have a good overlap with the magnetic dipole resonance.

Conclusion

We reported the design of AlGaAs nanoantennas. We showed that by varying height and radius of the nanodisk we could obtain a strong magnetic dipole resonance in the near-IR wavelength range. We predicted a SHG efficiency larger than 10-3 from a single nanodisk using a pump intensity of I0=1GW/cm2 at a wavelength of 1675 nm.

Reference

1. A. Kinkhabwala, et. al., "Large single-molecule fluorescence enhancements produced by a bowtie nanoantenna," Nat. Photonics 3, 654–657 (2009).

2. K. Kneipp, et. al., "Single molecule detection using surface-enhanced Raman scattering (SERS)," Phys. Rev. Lett. 78, 1667–1670 (1997).

3. H. A. Atwater and A. Polman, "Plasmonics for improved photovoltaic devices," Nat. Materials 9, 205–213 (2010).

4. E. Boisselier and D. Astruc, "Gold nanoparticles in nanomedicine: preparations, imaging, diagnostics, therapies and toxicity," Chem. Soc. Rev. 38, 1759–1782 (2009).

5. J. C. Ginn, et. al., "Realizing optical magnetism from dielectric metamaterials," Phys. Rev. Lett. 108, 097402 (2012).

6. P. Albella, et. al., "Electric and Magnetic Field Enhancement with Ultralow Heat Radiation Dielectric Nanoantennas: Considerations for Surface-Enhanced Spectroscopies," ACS Photonics 1, 524–529 (2014).

7. A. B. Evlyukhin, et. al., "Demonstration of magnetic dipole resonances of dielectric nanospheres in the visible region," Nano Lett. 12, 3749–3755 (2012).

8. S. Person, et. al., "Demonstration of zero optical backscattering from single nanoparticles," Nano Lett. 13, 1806–1809 (2013).

9. M. R. Shcherbakov, et. al., "Enhanced Third-Harmonic Generation in Silicon Nanoparticles Driven by Magnetic Response," Nano Lett. 14, 6488–6492 (2014).

10. D. de Ceglia, et. al., "Role of antenna modes and field enhancement in second harmonic generation from dipole nanoantennas," Opt. Express 23, 1715 (2015).

Figures used in the abstract

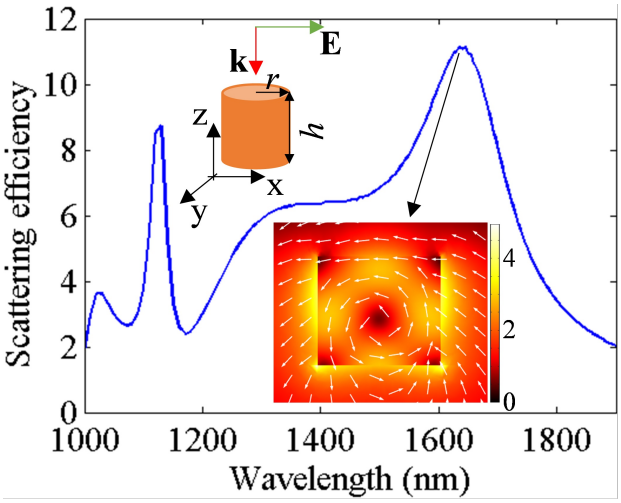

Figure 1: Scattering efficiency as a function of wavelength, calculated for r=225 nm and h=400 nm. A schematics of the AlGaAs cylinder with the incident field and the cross section of normalized |E| in the x-z plane through the axis of the cylinder are shown in the inset. The arrows represent E in the same x-z plane.

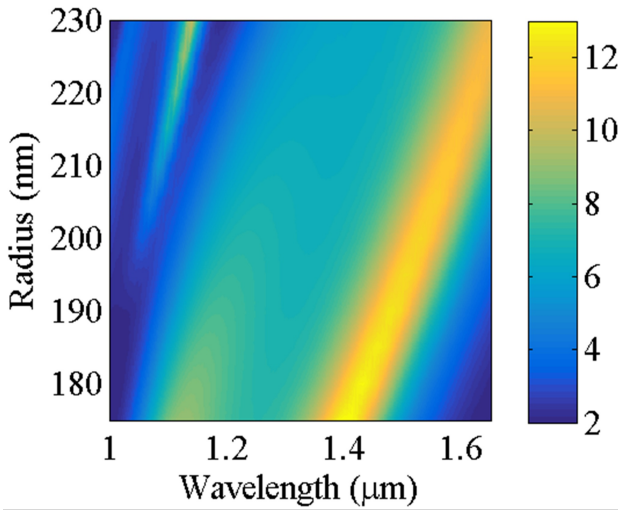

Figure 2: Scattering efficiency as a function of wavelength and cylinder radius for a constant height h=400 nm for cylinders suspended in air

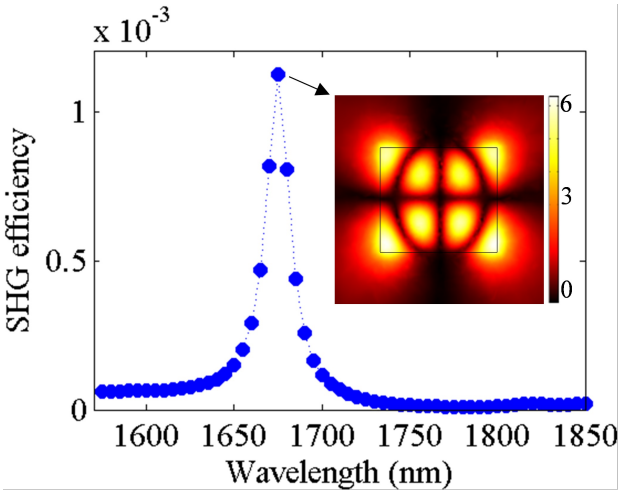

Figure 3: SHG efficiency as a function of pump wavelength for a cylinder with r=225 nm, h=400nm suspended in air and pump intensity I0=1GW/cm2. The normalized |ESH| on a cross section in the x-z plane at the center of the cylinder is shown in the inset.

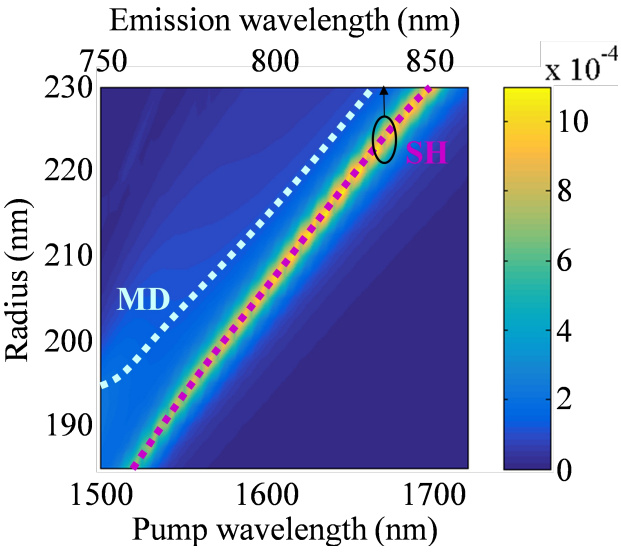

Figure 4: SHG efficiency as a function of pump wavelength and nanodisk radius. The magnetic dipole resonance (MD) and the resonant mode at the emission wavelength (SH) are outlined with a dotted white and magenta line respectively.